Activation of cGMP-Dependent Protein Kinase Restricts Melanoma Growth and Invasion by Interfering with the EGF/EGFR Pathway

JIDOpen

Marika Quadri[1,2], Antonella Comitato[2], Elisabetta Palazzo[1], Natascia Tiso[3], Andreas Rentsch[4], Giovanni Pellacani[1], Alessandra Marconi[1] and Valeria Marigo[2]

Drug resistance mechanisms still characterize metastatic melanoma, despite the new treatments that have been recently developed. Targeting of the cGMP/protein kinase G pathway is emerging as a therapeutic approach in cancer research. In this study, we evaluated the anticancer effects of two polymeric-linked dimeric cGMP analogs able to bind and activate protein kinase G, called protein kinase G activators (PAs) 4 and 5. PA5 was identified as the most effective compound on melanoma cell lines as well as on patient-derived metastatic melanoma cells cultured as three-dimensional spheroids and in a zebrafish melanoma model. PA5 was able to significantly reduce cell viability, size, and invasion of melanoma spheroids. Importantly, PA5 showed a tumor-specific outcome because no toxic effect was observed in healthy melanocytes exposed to the cGMP analog. We defined that by triggering protein kinase G, PA5 interfered with the EGF pathway as shown by lower EGFR phosphorylation and reduction of activated, phosphorylated forms of protein kinase B and extracellular signal–regulated kinase 1/2 in melanoma cells. Finally, PA5 significantly reduced the metastatic process in zebrafish. These studies open future perspectives for the cGMP analog PA5 as a potential therapeutic strategy for melanoma.

Journal of Investigative Dermatology (2021) ■, ■–■; doi:10.1016/j.jid.2021.06.011

INTRODUCTION

Melanoma is one of the most aggressive, complex, and deadliest types of cancer (Andor et al., 2016), and its worldwide incidence has been increasing annually at a more rapid rate than any other type of cancer (Ali et al., 2013). Improvements in diagnostic strategies allow most patients with melanoma to be diagnosed at an early stage and to be effectively treated with surgery. Nevertheless, approximately 20% of melanoma cases are diagnosed at an advanced stage, with a severe prognosis and lower probability of a sustained response to treatment (Luke et al., 2017). The therapeutic options for metastatic melanoma consist of chemotherapy, radiotherapy, immunotherapy, and targeted therapy (principally inhibitors of BRAF and MAPK/extracellular signal–regulated kinase [ERK]), which can be administered as single agents or in combination (Kozar et al., 2019). Although recent therapeutic strategies have increased overall patient survival, the prognosis for metastatic melanoma remains dismal owing to the occurrence of resistance mechanisms (Cosgarea et al., 2017; Rodríguez-Cerdeira et al., 2017). Given this evidence, there is an elevated medical need for new therapeutic strategies.

cGMP is a ubiquitous second messenger that mediates several intracellular signaling pathways by binding to specific targets (Rehmann et al., 2007). cGMP-dependent protein kinases (protein kinase Gs [PKGs]) are major downstream transducers of the cGMP signaling cascade (Rainer and Kass, 2016). The cGMP/PKG signaling pathway has been linked to numerous cellular processes, including proliferation, differentiation, and apoptosis (Francis et al., 2010; Power et al., 2020). Two types of PKG are expressed in mammalian cells, which have distinct subcellular localization, tissue expression, and substrates: the cytosolic PKG-I, which exists in two isoforms (Iα and Iβ) and the membrane-bound PKG-II (Sellak et al., 2013). In cancer, the participation of the cGMP/PKG pathway appears to be controversial. On the one hand, cGMP has been implicated in the regulation of growth and survival of multiple cell types, including tumor cells (Fajardo et al., 2014). On the other hand, the activation of the cGMP/PKG pathway has antitumor and pro-apoptotic effects in different cancer cell lines (Hoffmann et al., 2017; Fallahian et al., 2012; Karakhanova et al., 2014; Tuttle et al., 2016; Vighi et al., 2018; Wang et al., 2015; Windham and Tinsley, 2015; Wu et al., 2019, 2018). Specifically, overexpression of PKG-Iβ and, to a lesser extent, of PKG-Iα induced apoptosis in colon cancer (Deguchi et al., 2004, 2002).

The role of the cGMP/PKG pathway is not well-understood in melanoma. Arozarena et al. (2011) correlated the down-regulation of *PDE5A* gene in BRAFv600E-expressing melanoma cells with high intracellular levels of cGMP and

[1]*DermoLab, Department of Surgical, Medical, Dental and Morphological Science, University of Modena and Reggio Emilia, Modena, Italy;* [2]*Department of Life Sciences, University of Modena and Reggio Emilia, Modena, Italy;* [3]*Laboratory of Developmental Genetics, Department of Biology, University of Padua, Padua, Italy; and* [4]*BIOLOG Life Science Institute. Forschungslabor und Biochemica-Vertrieb, Bremen, Germany*

Correspondence: Alessandra Marconi, DermoLab, Department of Surgical, Medical, Dental and Morphological Sciences, University of Modena and Reggio Emilia, via Del Pozzo 71, 41124 Modena, Italy. E-mail: alessandra.marconi@unimore.it

Abbreviations: 3D, three-dimensional; ERK, extracellular signal–regulated kinase; PA, protein kinase G activator; PKG, protein kinase G; PLD, polymeric-linked dimeric; VASP, vasodilator stimulated phosphoprotein

Received 14 January 2021; revised 7 May 2021; accepted 18 June 2021; accepted manuscript published online XXX; corrected proof published online XXX

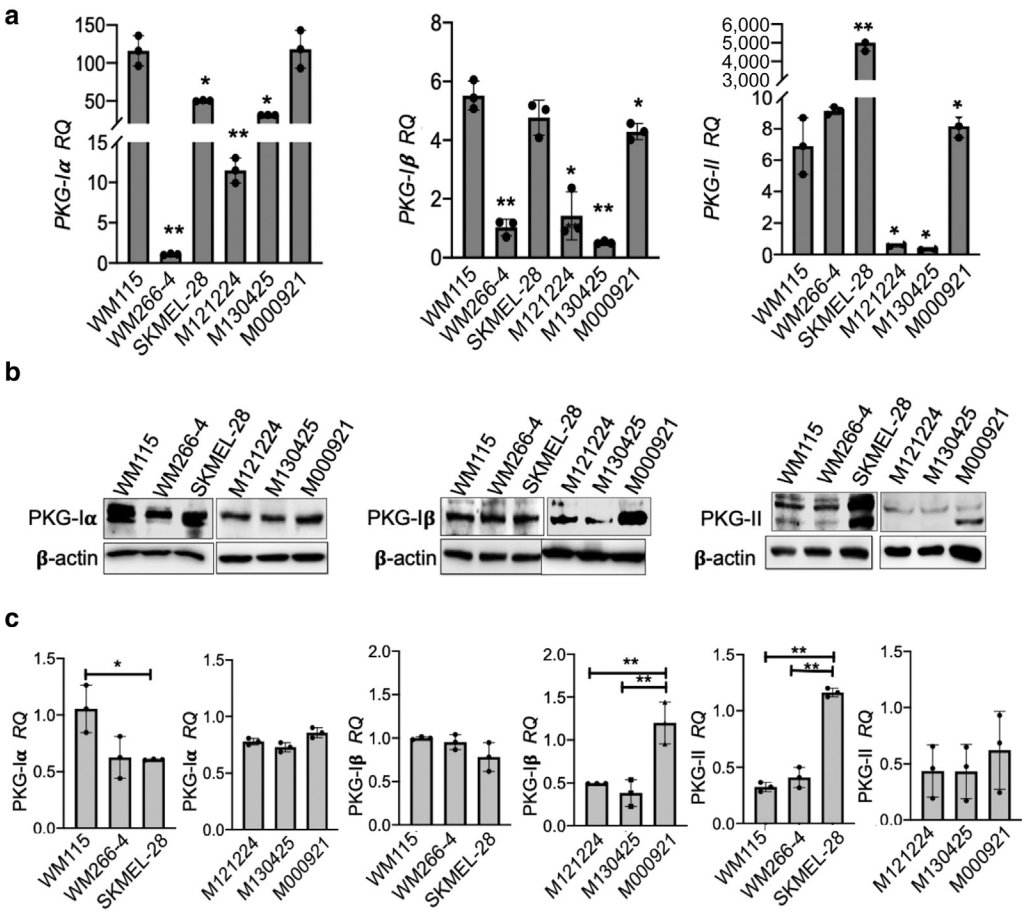

Figure 1. Expression of PKG isoforms in melanoma spheroids. (**a**) RQs of the *PKG-Iα*, *PKG-Iβ*, and *PKG-II* mRNAs were assessed by real-time qPCR in melanoma cell lines (WM115, WM266-4, and SKMEL-28) and human metastatic (M121224, M130425, and M000921) derived spheroids. *RPS26* was used as a reference gene. RQ of WM266-4 was set as 1 for *PKG-Iα* and *PKG-Iβ*, whereas the value of M130425 was set as 1 for *PKG-II*. Data represent the mean ± SD of triplicate determinations. Statistical analysis by one-way ANOVA was performed comparing the mRNA level of each sample with WM115 mRNA level. (**b**) Immunoblotting for PKG isoforms. (**c**) Quantification of PKG-Iα, PKG-Iβ, and PKG-II RQ was performed by ImageJ using β-actin as a normalizing protein. Data represent the mean ± SD of three independent biological experiments. Statistical analysis by one-way ANOVA was performed comparing the protein level of each sample with WM115 or M000921 protein levels. $^{**}P < 0.01$; $^{*}0.01 < P < 0.05$. PKG, protein kinase G; RQ, relative quantity.

melanoma cell invasion. Specific activation of the cGMP/PKG-I pathway was shown to promote MAPK signaling and melanoma growth in vitro and in vivo (Dhayade et al., 2016). We have recently shown that the activation of PKG-II by two polymeric-linked dimeric (PLD) cGMP analogs, the PKG activator (PA) 4 and 5, could reduce melanoma cell viability and mobility. Nevertheless, the specific function of the cGMP/PKG-II pathway needs to be clarified to facilitate its development as a potential therapy for melanoma.

The aim of this study was to validate the effects of the synthetic PDL cGMP analogs, PA4 and PA5, on in vitro melanoma models using three-dimensional (3D) cultures. For this purpose, we employed both melanoma cell lines and human metastatic melanoma cells. We provide evidence that the activation of PKG by PA5 reduces cell viability by inducing cell death and decreases growth area and invasion ability of melanoma spheroids. In detail, we show that PA5-dependent PKG activation is able to repress MAPK and phosphoinositide 3-kinase/protein kinase B pathways. Finally and most importantly, the antimetastatic effect of the PLD cGMP analog PA5 was confirmed in the zebrafish melanoma model.

RESULTS

PKG isoforms are differentially expressed in spheroids derived from melanoma cell lines and from patients' metastatic cells

To evaluate the influence of the culture method on PKG expression, PKG-Iα, PKG-Iβ, and PKG-II levels were analyzed in melanoma cell lines cultured in two-dimensional and 3D conditions (Supplementary Figure S1a–c). No major differences at mRNA and protein levels were observed between two-dimensional culture and 3D culture. Therefore, given that the 3D culture better recapitulates the features of the tumor in vivo (Marconi et al., 2018), all subsequent experiments were performed on melanoma spheroids. Given the genotypic and phenotypic heterogeneity of melanoma, we used different melanoma cell lines and primary metastatic melanoma cells, as described in Supplementary Table S1. We found significant differences in PKG isoform mRNA and protein levels among melanoma spheroids (Figure 1a–c). High amounts of PKG-Iα protein were found in WM115 compared with those in spheroids derived from the other melanoma cell lines, whereas all types of patient's metastatic spheroids expressed the PKG-Iα isoform at similar levels. In contrast, PKG-1β expression was significantly higher in M000921 than in other metastatic spheroids, whereas PKG-II was most abundant in the SKMEL-28 cell line.

The cGMP analog PA5 decreases proliferation and induces apoptosis in melanoma spheroids

We recently characterized two PLD cGMP analogs (PA4 and PA5) as PKG-II activators able to reduce cell viability in MNT1 and SKMEL-28 melanoma cell lines cultured in adherent conditions (Vighi et al., 2018). Now, we analyzed the effects of these compounds in 3D melanoma cell

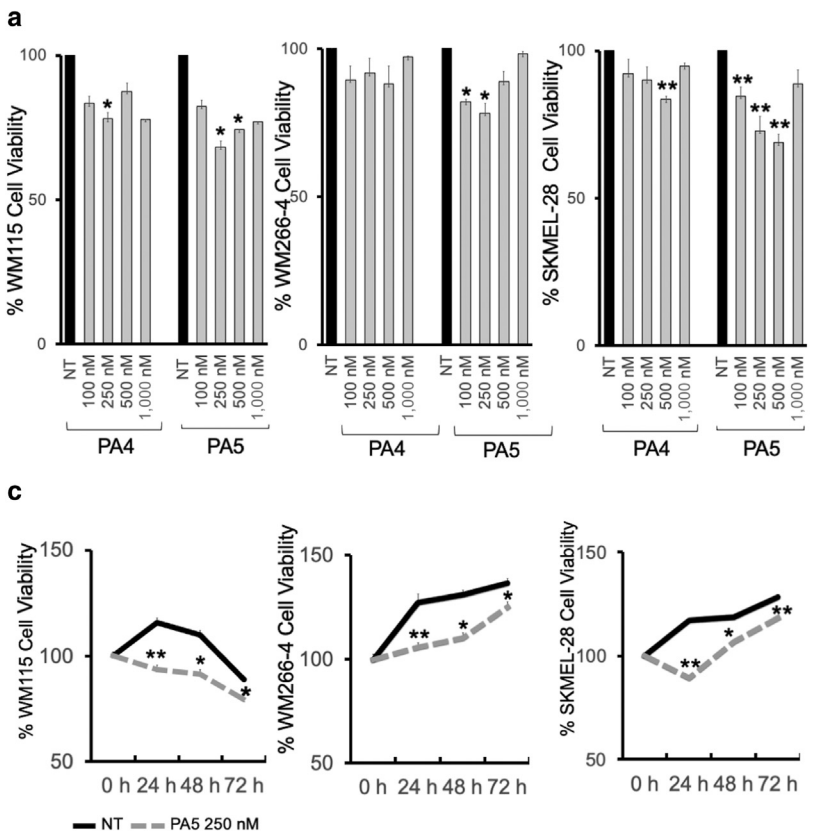

Figure 2. Cell viability after treatment with cGMP analogs in melanoma spheroids and human melanocytes. (**a**) Dose–response relationships of melanoma cell spheroids viability after exposure to different doses of PA4 and PA5 for 24 h. Values of NT cells were set as 100% of cell viability. (**b**) Cell viability in human metastatic melanoma spheroids treated with PA5 (250 nM) for 24 h. Values of NT cells were set as 100% of cell viability. (**c**) Viability time course of melanoma cell line–derived spheroids treated with PA5 (250 nM). Cell viabilities at each time point were expressed as a percentage compared with that of time 0. (**d**) PA5 toxicity was evaluated in human primary melanocytes by MTT assay. Values of NT cells were set as 100% of cell viability. Data represent means ± SD of triplicate determinations. Student's *t*-test was applied for statistical analyses of PA5-treated samples compared with NT. $^{**}P < 0.01$; $^{*}0.01 < P < 0.05$. h, hour; NT, not treated; PA, protein kinase G activator.

cultures. WM115, WM266-4, and SKMEL-28 spheroids were treated for 24 hours with scaling doses of PA4 and PA5 (100, 250, 500, and 1,000 nM) (Figure 2a). Whereas PA5 reduced cell viability in all melanoma spheroids, PA4 was only effective on WM115 and SKMEL-28 spheroids. Moreover, PA5 (250 nM) efficacy was confirmed in human metastatic derived spheroids after 24 hours of treatment (Figure 2b).

To further evaluate the efficacy of PA5, cell viability of WM115, WM266-4, and SKMEL-28 spheroids were analyzed 24 and 72 hours after PA5 treatment (Figure 2c). PA5 significantly decreased cell viability in all melanoma spheroids at all time points. Interestingly, no effect was detected after 24 hours of treatment in human melanocytes exposed to different doses (from 100 nM to 1,500 nM) of PA5 (Figure 2d). Given these results, PA5 (250 nM) was selected for further studies.

One of the downstream targets of PKG is vasodilator stimulated phosphoprotein (VASP), whose activities depend on phosphorylation at two main sites: serine 239 and serine 157. Whereas serine 157 is the main target of cAMP-dependent protein kinase (protein kinase A), PKGs preferentially phosphorylate VASP at serine 239 (Döppler and Storz, 2013). We detected phosphorylated VASP at serine 239 in melanoma spheroids after PA5 treatment using immunofluorescence and immunoblotting, confirming the activation of PKGs by PA5 (Supplementary Figure S2a–d). We ruled out the hypothesis of an off-target effect on protein kinase A by showing no change in the phosphorylation of VASP at serine 157 (Supplementary Figure S2c and d). We evaluated the spheroid growth area 24 and 72 hours after PA5 treatment (Figure 3a and b), showing that the activation of PKG by PA5 significantly reduced spheroid occupied areas at each time point, compared with the occupied areas in the untreated control (Figure 3b). To understand whether the decreased spheroid area was dependent on cell death, dying cells were detected by propidium iodide assay on melanoma spheroids 24 and 72 hours after PA5 treatment. PA5 increased the number of dead cells compared with that in the untreated samples in all melanoma spheroids, suggesting that induction of cell death in response to PKG activation is triggered by PA5 (Figure 3c).

PKG activation by PA5 decreases the invasion and survival of melanoma spheroids

To assess whether PA5 affects the invasive capacity of melanoma cells, spheroids were implanted in a matrix of collagen I, which mimics the extracellular microenvironment of the tumor in vivo. Spheroids were then treated with PA5 from 24 up to 72 hours and were photographed every 24 hours (Figure 4a). The percentage of fragmentation, which represents single or clustered cells released from the total spheroid, was calculated as described in Supplementary Materials and Methods. The percentage of fragmentation (Figure 4b) as well as the invasion area (Figure 4c) of spheroids were significantly lower in PA5-treated spheroids than in the controls. In addition, PA5 decreased the distance reached by migrating cells (Figure 4d).

To further confirm the effect of PA5 on melanoma spheroids viability and invasion, we evaluated the expression of

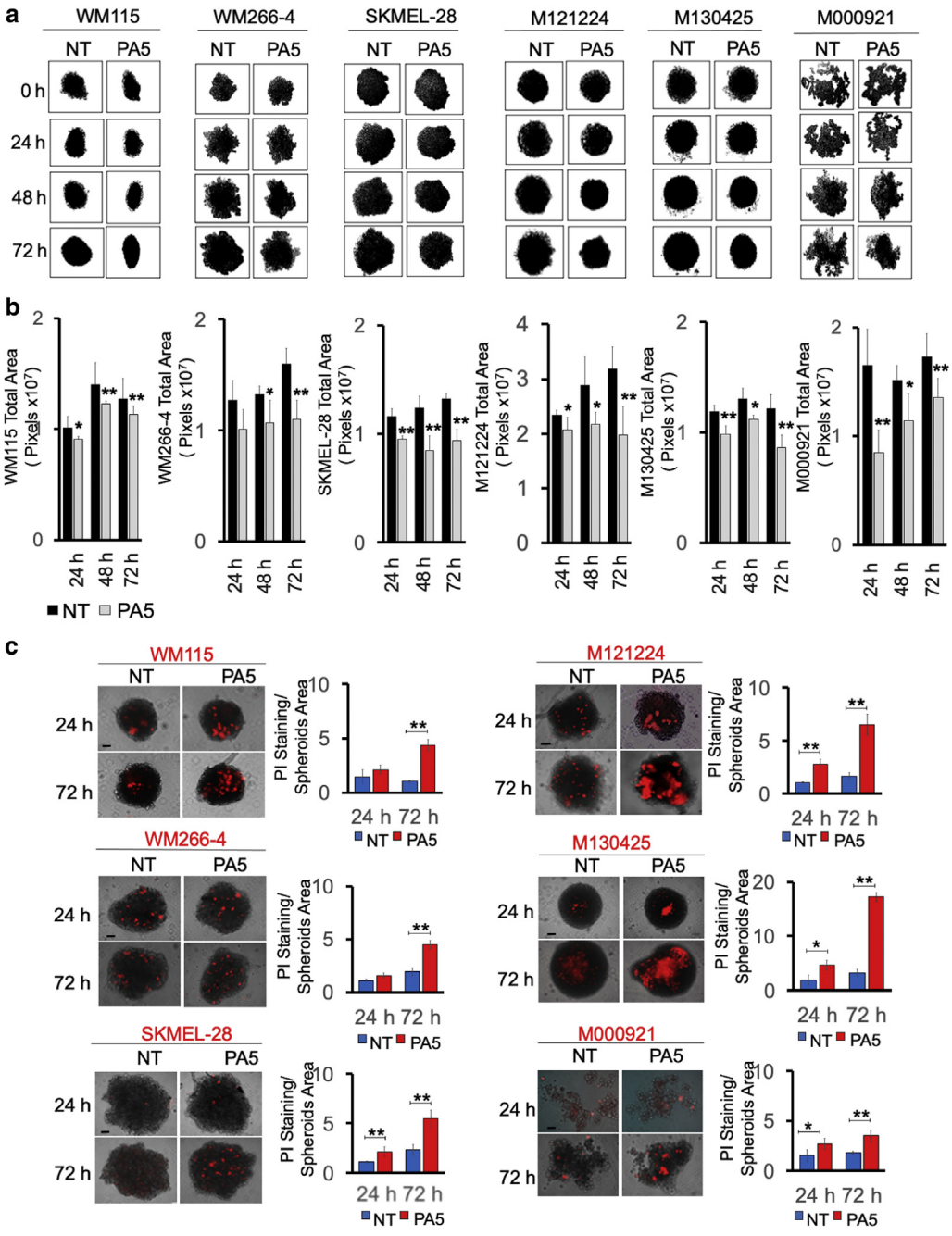

Figure 3. Effect of PA5 on melanoma viability. Melanoma spheroids were treated with PA5 from 24 to 72 h. (**a**) Pictures of spheroids taken at different time points. (**b**) Total areas occupied by spheroids were evaluated by ImageJ software. (**c**) Melanoma spheroids were treated with PA5 (250 nM), and dying cells were stained with PI at 24 and 72 h. Quantification of dying cells is presented as PI staining/ spheroids area. Bars = 100 μm. Data represent means of at least three spheroids ± SD of triplicate biological experiments. Student's *t*-test was used for statistical analyses of PA5-treated samples compared with NT. $^{**}P < 0.01$; $^{*}0.01 < P < 0.05$. h, hour; NT, not treated; PA, protein kinase G activator; PI, propidium iodide.

BIRC5 mRNA encoding Survivin, which is considered a biomarker of poor prognosis in melanoma (Takeuchi et al., 2005), *CXCL8*, which promotes cancer progression and invasion (Ugurel et al., 2001), and p21, encoded by the *CDKN1A* gene, a key negative regulator of cell cycle progression at the G1/G2 level (Yanagi et al., 2017). *BIRC5* and *CXCL8* mRNA levels significantly decreased in SKMEL-28 and M121224 spheroids treated with PA5, compared with the levels in the untreated ones. The interference of PKG activation with cell cycle progression was confirmed by the significant increase of *CDK1NA* mRNA in treated spheroids (Figure 4e and f). In addition, PA5 significantly increased BIM, a pro-apoptotic protein, and decreased the expression of Survivin (Figure 4g and h) in SKMEL-28 spheroids. Taken together, these results confirm that PA5 reduces melanoma spheroid cell invasion as well as growth and survival, possibly by activating apoptotic mechanisms.

Metastatic melanoma cells treated with PA5 fail to metastasize in zebrafish

Zebrafish has recently emerged as one of the most valid models for drug screening in vivo (Bootorabi et al., 2017; MacRae and Peterson, 2015). To confirm PA5 efficacy, M121224 and M130425 metastatic melanoma cells were stained with a viable dye and were injected in zebrafish *nacre* larvae (Figure 5a and b and Supplementary Figure S3a). At 72 hours later, zebrafish larvae were injected with scaling doses

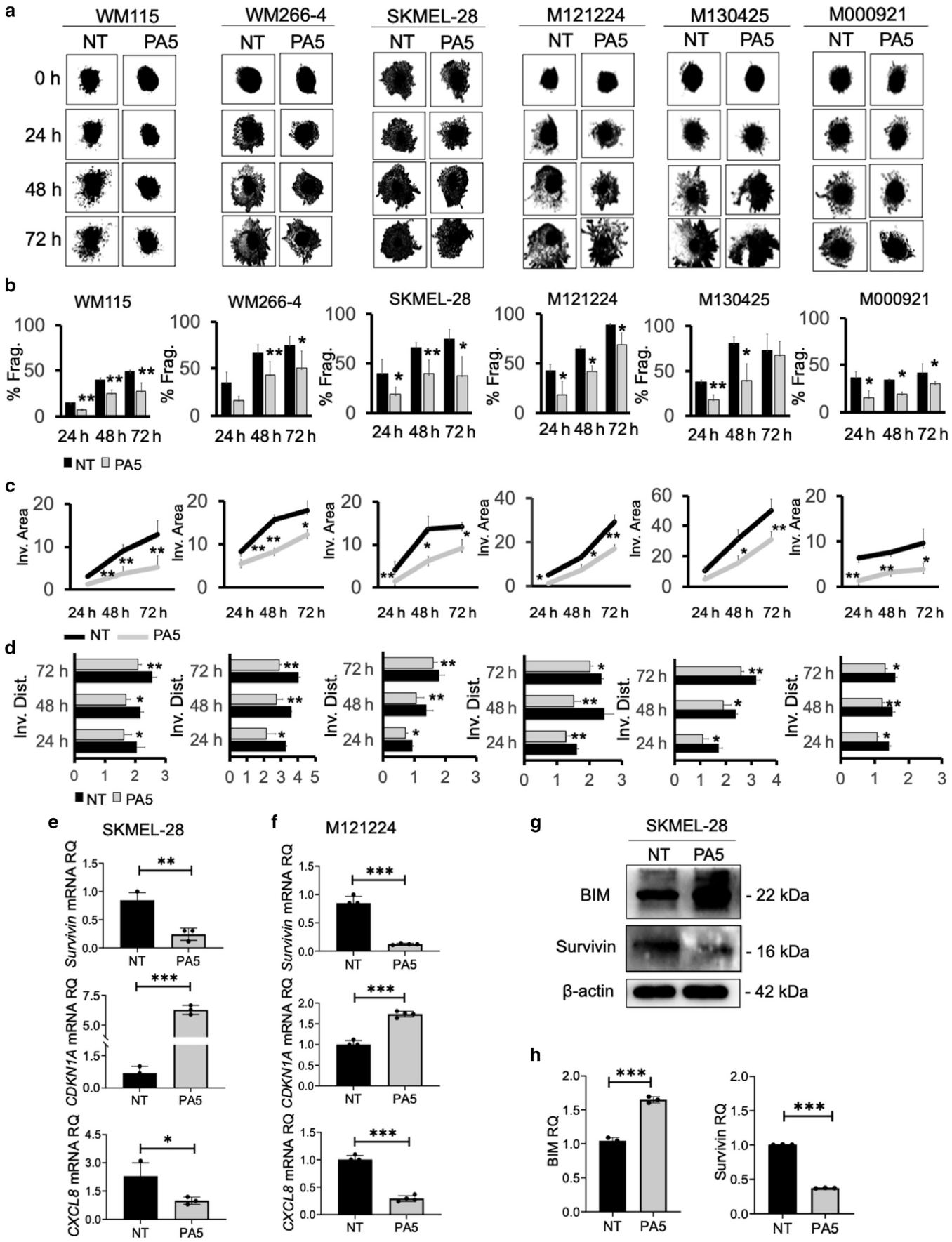

Figure 4. Effect of PA5 on melanoma spheroids invasion and survival. Melanoma spheroids were transferred onto a type I collagen matrix. At 24 h later, spheroids were treated with PA5. (**a**) Pictures of treated or NT spheroids were taken every 24 h up to 72 h. (**b**) Histograms representing the % Frag. of PA5-treated

of PA5 (0 nM, 500 nM, or 1,000 nM) into the yolk and were monitored from 4 days after cell injection up to 7 days after cell injection, that is, 4 days after treatment (Supplementary Figure S3b). No major increase in mortality was observed in zebrafish treated with both doses of PA5, compared with that observed in those not injected or in control zebrafish (Figure 5c). Although cells were confined to the site of injection in zebrafish 3 days after cell injection (Figure 5b), they spread in distant organs with time, and metastases were mainly classified as full and initial metastases in control injected fish 7 days after cell injection (4 days after treatment) (Figure 5d and e). PA5 treatment (500 nM) was able to decrease metastases, with about 40/50% of zebrafish showing only initial metastases and 50%/60% of zebrafish having cells at the site of injection (in place). The metastatic trend was completely reversed in larvae treated with 1,000 nM PA5, where about 78% of zebrafish showed only cells in place. We also observed a reduction of melanoma cell mass in treated fish. To substantiate this assumption, fluorescence intensity emitted by labeled injected cells was quantified by ImageJ software (National Institutes of Health, Bethesda, MD). As expected, PA5 significantly reduced fluorescence intensity in treated fish, compared with that in the control (Figure 5f), suggesting an inhibiting effect of the cGMP analog on cell growth.

PA5 inhibits the EGF/EGFR signaling cascade

Antiproliferative and pro-apoptotic effects have been linked to PKGII activation in different cell lines (Wu et al., 2019, 2018, 2017). We previously showed that PA5 could reduce cell viability by activating PKGII rather than PKGI (Vighi et al., 2018), but the exact mechanism remained to be clarified. PKGII has been previously demonstrated to reduce proliferation and activate apoptosis by inhibiting the EGF signaling, interfering with the MAPK/ERK- and phosphoinositide 3-kinase/protein kinase B–mediated pathways (Wu et al., 2019, 2018, 2017). To assess the effect of PA5 on EGFR signaling pathway, we focused on the SKMEL-28 cell line and M121224 metastatic cells, where a persistent stable response to PA5 was observed (Figures 3 and 4). SKMEL-28 and M121224 cells were pretreated with PA5 (250 nM) for 4 hours before stimulation with EGF (200 ng/ml). A higher phosphorylation of EGFR (phosphorylated EGFR) at Tyr-1068 confirmed that the cells could respond to EGF, whereas PA5 significantly blocked EGFR phosphorylation (Figure 6a–c). We then evaluated two of the downstream transducers of the EGF pathway, that is, protein kinase B and ERK1/2 (phosphorylated ERK1/2), which are phosphorylated in response to EGF signaling (phosphorylated protein kinase B and phosphorylated ERK1/2). Phosphorylation of both EGF mediators was significantly lower after PA5 exposure (Figure 6a and d). Moreover, Cyclin B1, N-cadherin, and BIM levels were also affected in M121224 cells 24 hours after PA5 treatment (Figure 6e and f). In fact, increased levels of Cyclin B1 and N-cadherin, induced by EGF, were completely reverted by PA5. In contrast, the reduced levels of the pro-apoptotic factor BIM were significantly recovered by PA5. Altogether, these results strongly suggest that PKG activation inhibits the EGFR pathway in melanoma.

DISCUSSION

Melanoma is one of the most aggressive and heterogeneous types of cancer, being highly refractory to conventional chemotherapy (Andor et al., 2016). Recently, we identified two PLD cGMP analogs (PA4 and PA5) as unidentified compounds able to reduce cell viability in melanoma cell lines cultured in two-dimensional conditions, and their effects were associated with the activation of PKG-II (Vighi et al., 2018). To assess the therapeutic potentials of such PKG activators, we extended the study to 3D melanoma models, by including cell lines and primary melanoma metastases. We confirmed PA5 as the most effective compound because it highly reduced the viability of WM115, WM266-4, and SKMEL-28 melanoma spheroid by penetrating the complex spheroid structure. The poor effect observed with PA4 may reflect the fact that is not specific for PKG-II but can activate PKG-I, as shown by in vitro activity assays (Vighi et al., 2018). Compounds acting with similar association constant on PKG-II and PKG-I may thus favor melanoma cell growth and invasion on prevalent activation of one of the two PKG-I isoforms (Arozarena et al., 2011; Dhayade et al., 2016). A PKGIα-mediated protumorigenic effect was reported in lung (Leung et al., 2010) and ovarian (Hou et al., 2006) cancers, and overexpression of PKG-Iβ can be antineoplastic in breast (Fallahian et al., 2012) and colon (Lan et al., 2012) cancers. Conversely, the specific activation of PKG-II interfered with proliferation and triggered pro-apoptotic effects in several cancer cell lines (Hoffmann et al., 2017; Tuttle et al., 2016; Wu et al., 2019, 2018). We previously showed that MNT1 cells expressed low levels of PKG-Iα (Vighi et al., 2018), which is otherwise highly expressed in all melanoma spheroids employed in this study. Thus, we speculate that specific differential expression of PKG isoforms in different melanoma cells can lead to divergent responses on exposure to PKG activators. The null effect of PA4 on melanoma spheroids may be due to the possible activation of both PKG-Iα and PKG-II, and this may promote opposite compensatory effects. Conversely, PA5, more specific for PKG-II, significantly reduced cell viability, spheroid area, and invasion and increased the number of apoptotic cells in melanoma spheroids.

or -NT spheroids at each time point. (**c**) Graphs representing the changes of the Inv. areas of PA5-treated spheroids versus that of NT spheroids evaluated by the ImageJ software. (**d**) Histograms representing the Inv. Dist. reached by cells in treated versus those reached by NT spheroids. Data represent the means of at least three spheroids ± SD of triplicate biological experiments. Student's *t*-test was used for statistical analyses of PA5-treated samples compared with NT. (**e**) SKMEL-28– and (**f**) M121224-derived spheroids were treated with PA5 (250 nM) for 24 h, and the expression (RQ) of *BIRC5*, *CDKN1A*, and *CXCL8* mRNAs was evaluated by real-time qPCR. β-Actin was used as a reference gene. Data represent the mean ± SD of triplicate determinations. Student's *t*-test was used for statistical analysis. (**g**) BIM and Survivin protein levels in SKMEL-28 spheroids after PA5 treatment. (**h**) Protein levels (RQ) represented as mean of protein/β-actin ratio ± SD from three biological replicates. NT data were set as 1. Student's *t*-test was applied for statistical analysis. ***$P < 0.001$; **$0.001 < P < 0.01$; *$0.01 < P < 0.05$. % Frag., percentage of fragmentation; Dist., distance; h, hour; Inv., invasion; NT, not treated; PA, protein kinase G activator; RQ, relative quantity.

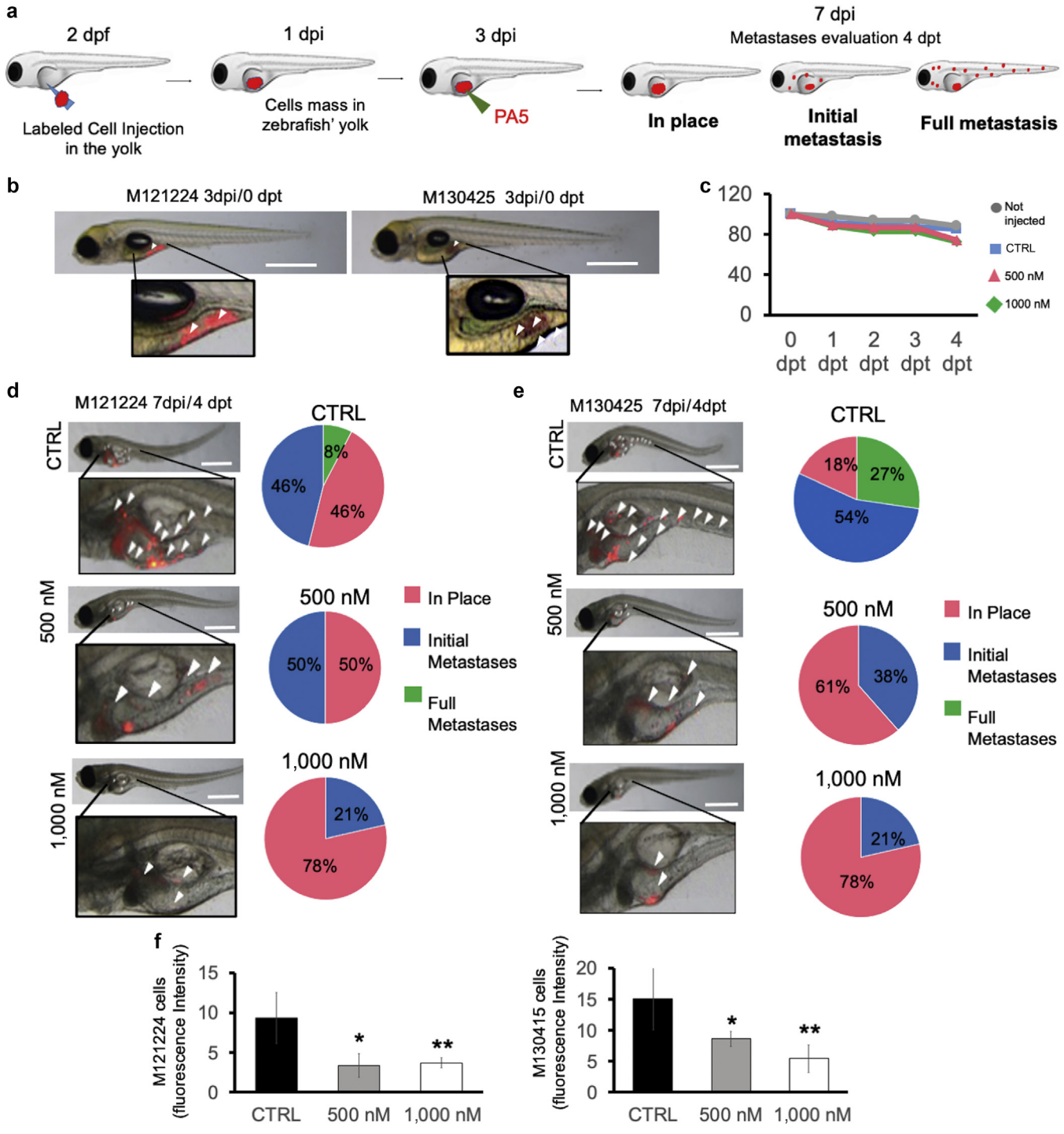

Figure 5. Metastasis repression by PA5 in zebrafish melanoma models. (**a**) Metastatic cells were labeled with a viable dye and were injected in the zebrafish yolk at 2 dpf. One day after cell injection, zebrafish displaying cells in the circular vessels were discarded. Three days after cell injection, a solution of PA5 (500 nM or 1,000 nM) was injected into the zebrafish yolk. Zebrafish were monitored until 4 dpt (7 dpi). Metastases were classified as follows: (i) in place, cells confined to the site of injection; (ii) initial metastases, cells spread from the yolk to near organs (heart, swim bladder, and pharynx); and (iii) full metastases, cells in distant organs, such as brain, skeletal muscle, and trunk. (**b**) M121224- and M130425-labeled cells (red) are shown at the time of PA5 injection. Bar = 1 mm (**c**) Zebrafish were monitored each day up to 4 dpt (7 dpf) to evaluate the mortality rate after treatment. The number of fish on 0 dpt were set as 100% of zebrafish viability. (**d, e**) Localization of the stained cells (red, indicated with white arrows) was evaluated, and the metastasis was quantified. Bar = 1 mm. (**f, g**) Cell fluorescence intensities were measured by ImageJ software and normalized on cell fluorescence at time 0. Data represent the means ± SD of three independent biological experiments. Student's *t*-test was used for statistical analyses. $^{**}P < 0.01$; $^{*}0.01 < P < 0.05$. CTRL, control; dpf, days post fertilization; dpi, days post-injection; dpt, days post-treatment; PA, protein kinase G activator.

Importantly, PA5 had no negative effect on healthy melanocytes, suggesting that this compound could act on the cGMP/PKG pathway only in a tumoral context.

Overexpression of EGF and EGFR correlates with metastases, resistance to chemotherapy, and poor prognosis of numerous types of cancer (Lemmon and Schlessinger et al.,

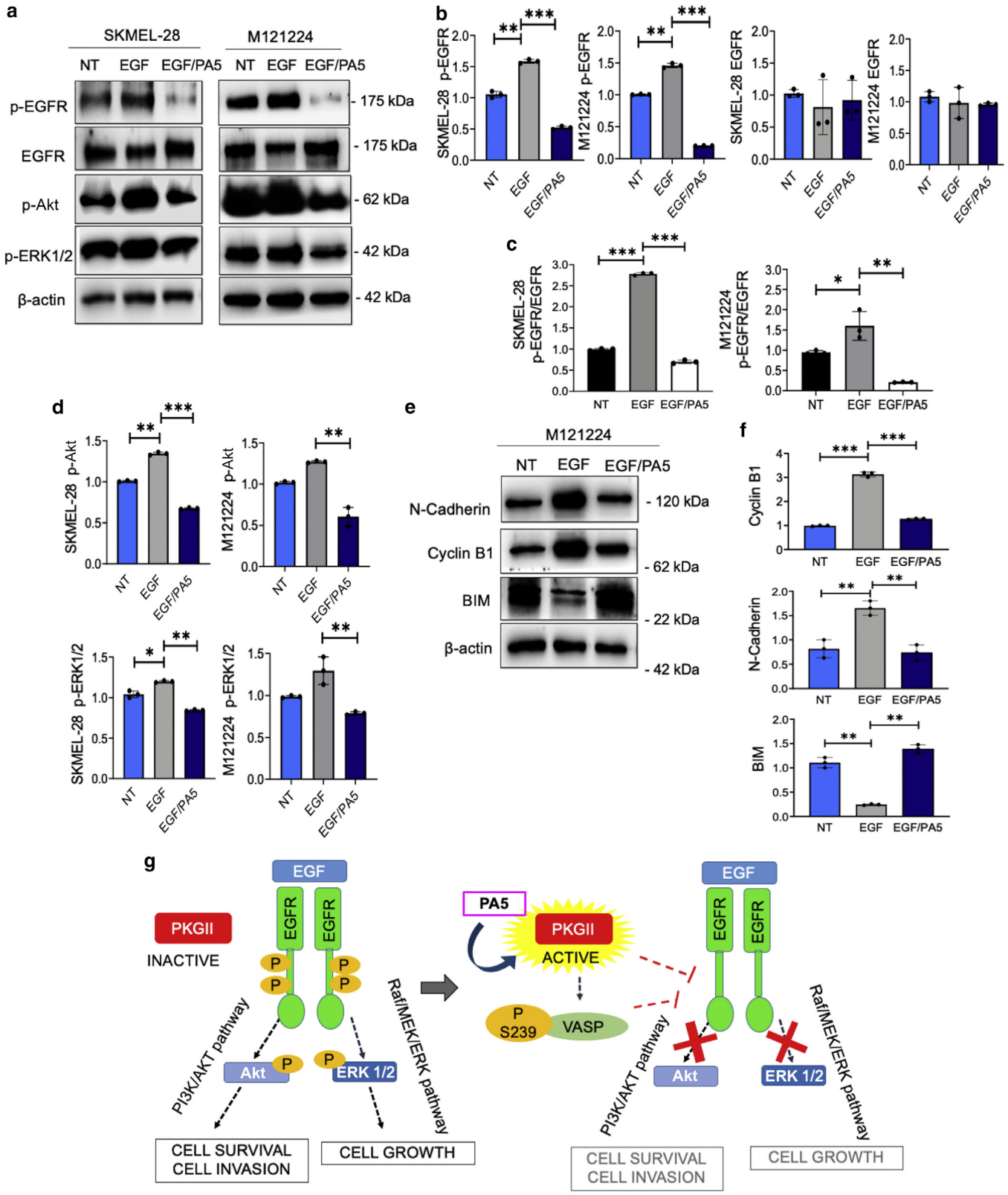

Figure 6. PKG activation by PA5 interferes with the EGF/EGFR pathway. SKMEL-28 and M121224 cells were serum starved for 24 hours, treated with PA5 for 4 hours, and then stimulated with EGF for 30 minutes. (**a**) Immunoblotting of p-EGFR, EGFR, p-Akt, p-ERK1/2 after exposure to EGF or to EGF together with PA5. (**b**) RQ of protein levels of p-EGFR and EGFR were calculated by ImageJ software using β-actin as a normalizer. (**c**) The p-EGFR-to-EGFR ratio was calculated using ImageJ data. (**d**) Protein levels (RQ) of p-Akt and p-ERK1/2 were calculated by ImageJ software using β-actin as a normalizer. (**e**) Immunoblotting of N-cadherin, Cyclin B1, and BIM proteins in M121224 cells 24 hours after EGF and PA5 treatment. (**f**) Proteins levels (RQ) of N-cadherin, Cyclin B1, and BIM were measured by ImageJ software using β-actin as a normalizer. Data represent the means ± SD of three independent biological experiments. Student's *t*-test was used for statistical analyses, and *P*-value was calculated referring to the EGF level. ***$P < 0.001$; **$0.001 < P < 0.01$; *$0.01 < P < 0.05$. (**g**) Schematic

2010). In this study, we showed, to our knowledge previously unreported, that activation of PKGII interferes with the EGF/EGFR pathway in melanoma (Figure 6g). The EGFR pathway participates in the regulation of cell proliferation, cell invasion, and prevention from apoptosis (Di Domenico and Giordano, 2017). The reduction of the cell cycle protein Cyclin B1 and of the adhesion molecule linked to epithelial-to-mesenchymal transition, N-cadherin, (Gheldof and Berx, 2013) as well as the increase of BIM pro-apoptotic protein, observed after treatment with PA5, are potential consequences related to the inhibition of the EGF pathway. In addition, VASP could be a key mediator, because this protein was shown to interfere with EGFR and MAPK/ERK signal transduction in lung cancer cells on phosphorylation in serine 239 by PKG (Di Domenico and Giordano, 2017). Further studies are required to define whether PKGII acts directly on EGFR or indirectly through VASP.

One of the most important results in this study was the demonstration of the antimetastatic effect of PA5 in vivo. The advantage of using zebrafish resides in the availability of transparent albino strains (*casper or nacre*) that allows an in vivo and real-time improved imaging of labeled injected cells for the study of cancer cell invasion and interaction with the microenvironment (Heilmann et al., 2015; Kim et al., 2017). Despite that 70% of the human genes have an ortholog in the zebrafish genome, differences exist between human and fish organ systems (Lieschke and Currie, 2007; Howe et al., 2013). Although larvae can perform metabolism reactions and their drug distribution, metabolism, excretion, and allocation are similar to those of the human system, this is an area still under investigation in zebrafish. Nevertheless, zebrafish is increasingly recognized as a model for the prescreening of drugs and disease studies (MacRae and Peterson, 2015; Tavares and Santos Lopes, 2013). PA5 confirmed its antimetastatic effect in about 80% of treated fish, with a reduction of melanoma cell mass in treated fish, compared with that in the control. On the basis of our in vitro study, we hypothesize that the reduction of metastases in zebrafish may be due to the inhibition of cell growth and invasion. These data substantiate the efficacy of this compound in a more physiological context with no in vivo toxicity observed at two doses of PA5. Given the rapid metabolism of cyclic nucleotides, one can envision a limitation in the use of such compound. However, appropriate formulations can overcome such a problem. In fact, we previously showed that the bioavailability of a cGMP analog, CN03, could be highly improved on encapsulation of the compound in a liposome when injected into rats (Vighi et al., 2018).

In summary, we showed the antiproliferative and anti-invasive effect of a PKG-II activator in melanoma. We also provided evidence that the molecule acts, at least in part, through the inhibition of the EGFR pathway. Because the EGFR pathway is activated in advanced stages of melanoma and in acquired resistance to BRAF inhibitors (Gross et al., 2015), the prospective use of this PLD cGMP analog can open new opportunities for melanoma treatment. Future studies will focus on the use of this PDL cGMP analog as an alternative to current therapies and in target- and chemo-resistant melanomas.

MATERIALS AND METHODS

Cell cultures

Melanoma cell lines (WM115, WM266-4, and SKMEL-28) were obtained from the ATCC (Manassas, VA). Human metastatic melanoma cells (M121224, M130425, and M000092) were generously donated by M. Levesque of the University of Zurich (Switzerland) and were obtained from the University Research Priority Program melanoma biobank Zurich according to ethics approval BASEC-Nr.2017-00494. Human primary melanocytes were obtained from surplus healthy human tissue from the Operating Room of the Policlinico in Modena (Italy) with patient-provided informed written consent approved by the Ethical Committee of Area Vasta Emilia Nord (Italy) (protocol number 118/2014/ Apr. 11/09/2014). Cells were cultured as reported in Supplementary Materials and Methods.

PA4 (cGMP-8-T-(EO)5-ET-8-cGMP) and PA5 (cGMP-8-TMAmd-(PEG-pd-2000)-AmdMT-8-cGMP) were synthesized by Biolog Life Science Institute (Bremen, Germany). Melanoma spheroids were obtained by the liquid overlay technique or the Ultra-Low-Attachment. 96-multiwell method (Corning, Amsterdam, Netherlands). MTT assay and propidium Iodide assays were performed to evaluate cell viability and apoptosis, as indicated in Supplementary Materials and Methods. Pictures of spheroids were analyzed by ImageJ software (National Institutes of Health) as previously indicated (Saltari et al., 2016).

Real-time qPCR and western blotting

Total RNA and total proteins were extracted from melanoma cells cultured in adherent conditions (two-dimensional) or as spheroids, as described in Supplementary Materials and Methods. The specific primers for *PRKG-I* variant α and β and *PRKG-II* and specific antibodies for immunoblotting are reported in the Supplementary Material and Methods and were used as previously published (Vighi et al., 2018). To evaluate the inhibition of the EGF/EGFR pathway, SKMEL-28 and M121224 metastatic cells were treated with PA5 for 4 hours, and EGF was added for 30 minutes and 24 hours.

Immunofluorescence

WM115, WM266-4, and SKMEL28 cells were cultured in 3D conditions and treated with PA5. After 24 hours, spheroids were disaggregated, fixed, and cytospinned as indicated in Supplementary Materials and Methods. Cells were incubated with the primary antibody phosphorylated VASP (Ser239) (1:250, Nanotools, Teningen, Germany) at 4 °C overnight and with antimouse IgG, Alexa Flour 546 (1:500, Thermo Fisher Scientific, Waltham, MA) for 45 minutes. Pictures were collected using the ZOEFluorescent Cell Imager (Bio-Rad Laboratories, Hercules, CA).

Collagen I invasion assay

Melanoma spheroids were implanted in a scaffold of type I collagen solution and treated with PA5. Spheroids were then monitored, and pictures were taken from 0 hours to 72 hours and analyzed with ImageJ software (National Institutes of Health). More details are reported in Supplementary Materials and Methods.

representation of the proposed molecular mechanism. ERK, extracellular signal–regulated kinase; MEK, MAPK/extracellular signal–regulated kinase; NT, not treated; PA, protein kinase G activator; p-Akt, phosphorylated protein kinase B; p-EGFR, phosphorylated EGFR; p-ERK, phosphorylated extracellular signal–regulated kinase; PKG, protein kinase G; PI3K, phosphoinositide 3-kinase; RQ, relative quantity.

Zebrafish melanoma model

Zebrafish handling was performed at the Zebrafish Centre of the University of Padua, Italy, in accordance with the European and Italian Legislations (Directive 2010/63/EU) and with permission for animal experimentation from the Ethics Committee of the University of Padua and the Italian Ministry of Health (Authorization number 407/2015-PR). Zebrafish embryos were obtained from natural spawning of nacre (*mitfaw2/w2*), raised following standard protocols (Kimmel et al., 1995). Xenotransplants procedure and treatment are fully described in the Supplementary Materials and Methods.

Statistics

Results are presented as mean ± SD from three independent experiments. Statistical analysis was performed with one-way ANOVA and Student's *t*-test with significance at $*0.01 < P < 0.05$, $**0.001 < P < 0.01$, or $***P < 0.001$.

Data availability statement

No datasets were generated or analyzed during this study.

ORCIDs

Marika Quadri: http://orcid.org/0000-0001-7619-660X
Antonella Comitato: http://orcid.org/0000-0001-9686-3852
Elisabetta Palazzo: http://orcid.org/0000-0002-0812-5524
Natascia Tiso: http://orcid.org/0000-0002-5444-9853
Andreas Rentsch: http://orcid.org/0000-0003-4792-131X
Giovanni Pellacani: http://orcid.org/0000-0002-7222-2951
Alessandra Marconi: http://orcid.org/0000-0002-5667-5766
Valeria Marigo: http://orcid.org/0000-0002-4428-2084

CONFLICT OF INTEREST

AR is an employee of Biolog Life Science Institute, which is selling the applied cGMP analogs as research reagents. The remaining authors state no conflict of interest.

ACKNOWLEDGMENTS

This work was supported by the European Union (DRUGSFORD; HEALTH-F2-2012-304963) to VM. NT was supported by the Associazione Italiana per la Ricerca sul Cancro grant IG 2017-19928 and the Telethon grant GGP19287. We thank Mitchell Levesque of the University Hospital of Zurich Biobank who kindly donated human metastatic melanoma cells (M121224, M130425, M0000921). We are grateful to Carlo Pincelli for constructive discussion. The DeBio Zebrafish Facility at the University of Padua (Italy) is also gratefully acknowledged.

AUTHOR CONTRIBUTIONS

Conceptualization: VM, AM, MQ; Data Curation: MQ, AC, EP; Formal Analysis: MQ, AM, VM; Funding Acquisition: VM, NT; Investigation: MQ, AC, EP, NT; Methodology: MQ, EP, AM; Resources: AM, VM; Writing - Original Draft Preparation: MQ, AM, VM; Writing - Review and Editing: MQ, AC, EP, NT, AR, GP, AM, VM

SUPPLEMENTARY MATERIAL

Supplementary material is linked to the online version of the paper at www.jidonline.org, and at https://doi.org/10.1016/j.jid.2021.06.011.

REFERENCES

Ali Z, Yousaf N, Larkin J. Melanoma epidemiology, biology and prognosis. EJC Suppl 2013;11:81–91.

Andor N, Graham TA, Jansen M, Xia LC, Aktipis CA, Petritsch C, et al. Pan-cancer analysis of the extent and consequences of intratumor heterogeneity. Nat Med 2016;22:105–13.

Arozarena I, Sanchez-Laorden B, Packer L, Hidalgo-Carcedo C, Hayward R, Viros A, et al. Oncogenic BRAF induces melanoma cell invasion by downregulating the cGMP-specific phosphodiesterase PDE5A. Cancer Cell 2011;19:45–57.

Bootorabi F, Manouchehri H, Changizi R, Barker H, Palazzo E, Saltari A, et al. Zebrafish as a model organism for the development of drugs for skin cancer. Int J Mol Sci 2017;18:45–57.

Cosgarea I, Ritter C, Becker JC, Schadendorf D, Ugurel S. Update on the clinical use of kinase inhibitors in melanoma. J Dtsch Dermatol Ges 2017;15:887–93.

Deguchi A, Soh JW, Li H, Pamukcu R, Thompson WJ, Weinstein IB. Vasodilator-stimulated phosphoprotein (VASP) phosphorylation provides a biomarker for the action of exisulind and related agents that activate protein kinase G. Mol Cancer Ther 2002;1:803–9.

Deguchi A, Thompson WJ, Weinstein IB. Activation of protein kinase G is sufficient to induce apoptosis and inhibit cell migration in colon cancer cells. Cancer Res 2004;64:3966–73.

Dhayade S, Kaesler S, Sinnberg T, Dobrowinski H, Peters S, Naumann U, et al. Sildenafil potentiates a cGMP-dependent pathway to promote melanoma growth. Cell Rep 2016;14:2599–610.

Di Domenico M, Giordano A. Signal transduction growth factors: the effective governance of transcription and cellular adhesion in cancer invasion. Oncotarget 2017;8:36869–84.

Döppler H, Storz P. Regulation of VASP by phosphorylation: consequences for cell migration. Cell Adh Migr 2013;7:482–6.

Fajardo AM, Piazza GA, Tinsley HN. The role of cyclic nucleotide signaling pathways in cancer: targets for prevention and treatment. Cancers (Basel) 2014;6:436–58.

Fallahian F, Karami-Tehrani F, Salami S. Induction of apoptosis by type Iβ protein kinase G in the human breast cancer cell lines MCF-7 and MDA-MB-468. Cell Biochem Funct 2012;30:183–90.

Francis SH, Busch JL, Corbin JD, Sibley D. cGMP-dependent protein kinases and cGMP phosphodiesterases in nitric oxide and cGMP action. Pharmacol Rev 2010;62:525–63.

Gheldof A, Berx G. Cadherins and epithelial-to-mesenchymal transition. Prog Mol Biol Transl Sci 2013;116:317–36.

Gross A, Niemetz-Rahn A, Nonnenmacher A, Tucholski J, Keilholz U, Fusi A. Expression and activity of EGFR in human cutaneous melanoma cell lines and influence of vemurafenib on the EGFR pathway. Target Oncol 2015;10:77–84.

Heilmann S, Ratnakumar K, Langdon EM, Kansler ER, Kim IS, Campbell NR, et al. A quantitative system for studying metastasis using transparent zebrafish. Cancer Res 2015;75:4272–82.

Hoffmann D, Rentsch A, Vighi E, Bertolotti E, Comitato A, Schwede F, et al. New dimeric cGMP analogues reduce proliferation in three colon cancer cell lines. Eur J Med Chem 2017;141:61–72.

Hou Y, Gupta N, Schoenlein P, Wong E, Martindale R, Ganapathy V, et al. An anti-tumor role for cGMP-dependent protein kinase. Cancer Lett 2006;240:60–8.

Howe K, Clark MD, Torroja CF, Torrance J, Berthelot C, Muffato M, et al. The zebrafish reference genome sequence and its relationship to the human genome [published correction appears in Nature 2014;505:248]. Nature 2013;496:498–503.

Karakhanova S, Golovastova M, Philippov PP, Werner J, Bazhin AV. Interlude of cGMP and cGMP/protein kinase G type 1 in pancreatic adenocarcinoma cells. Pancreas 2014;43:784–94.

Kim IS, Heilmann S, Kansler ER, Zhang Y, Zimmer M, Ratnakumar K, et al. Microenvironment-derived factors driving metastatic plasticity in melanoma. Nat Commun 2017;8:14343.

Kimmel CB, Ballard WW, Kimmel SR, Ullmann B, Schilling TF. Stages of embryonic development of zebrafish. Dev Dyn 1995;203:253–310.

Kozar I, Margue C, Rothengatter S, Haan C, Kreis S. Many ways to resistance: how melanoma cells evade targeted therapies. Biochim Biophys Acta Rev Cancer 2019;1871:313–22.

Lan T, Chen Y, Sang J, Wu Y, Wang Y, Jiang L, et al. Type II cGMP-dependent protein kinase inhibits EGF-induced MAPK/JNK signal transduction in breast cancer cells. Oncol Rep 2012;27:2039–44.

Lemmon MA, Schlessinger J. Cell signaling by receptor tyrosine kinases. Cell 2010;25:1117–34.

Leung EL, Wong JC, Johlfs MG, Tsang BK, Fiscus RR. Protein kinase G type Ialpha activity in human ovarian cancer cells significantly contributes to enhanced Src activation and DNA synthesis/cell proliferation. Mol Cancer Res 2010;8:578–91.

Lieschke GJ, Currie PD. Animal models of human disease: zebrafish swim into view. Nat Rev Genet 2007;8:353–67.

Luke JJ, Flaherty KT, Ribas A, Long GV. Targeted agents and immunotherapies: optimizing outcomes in melanoma. Nat Rev Clin Oncol 2017;14:463–82.

MacRae CA, Peterson RT. Zebrafish as tools for drug discovery. Nat Rev Drug Discov 2015;14:721–31.

Marconi A, Quadri M, Saltari A, Pincelli C. Progress in melanoma modeling in vitro. Exp Dermatol 2018;27:578–86.

Power M, Das S, Schütze K, Marigo V, Ekström P, Paquet-Durand F. Cellular mechanisms of hereditary photoreceptor degeneration – focus of cGMP. Prog Retin Eye Res 2020;74:100772.

Rainer PP, Kass DA. Old dog, new tricks: novel cardiac targets and stress regulation by protein kinase G. Cardiovasc Res 2016;111:154–62.

Rehmann H, Wittinghofer A, Bos JL. Capturing cyclic nucleotides in action: snapshots from crystallographic studies. Nat Rev Mol Cell Biol 2007;8:63–73.

Rodríguez-Cerdeira C, Carnero Gregorio M, López-Barcenas A, Sánchez-Blanco E, Sánchez-Blanco B, Fabbrocini G, et al. Advances in immunotherapy for melanoma: a comprehensive review. Mediat Inflamm 2017;2017:1–14.

Saltari A, Truzzi F, Quadri M, Lotti R, Palazzo E, Grisendi G, et al. CD271 down-regulation promotes melanoma progression and invasion in three-dimensional models and in zebrafish. J Invest Dermatol 2016;136:2049–58.

Sellak H, Choi CS, Dey NB, Lincoln TM. Transcriptional and post-transcriptional regulation of cGMP-dependent protein kinase (PKG-I): pathophysiological significance. Cardiovasc Res 2013;97:200–7.

Takeuchi H, Morton DL, Elashoff D, Hoon DSB. Survivin expression by metastatic melanoma predicts poor disease outcome in patients receiving adjuvant polyvalent vaccine. Int J Cancer 2005;117:1032–8.

Tavares B, Santos Lopes S. The importance of zebrafish in biomedical research. Acta Med Port 2013;26:583–92.

Tuttle TR, Mierzwa ML, Wells SI, Fox SR, Ben-Jonathan N. The cyclic GMP/protein kinase G pathway as a therapeutic target in head and neck squamous cell carcinoma. Cancer Lett 2016;370:279–85.

Ugurel S, Rappl G, Tilgen W, Reinhold U. Increased serum concentration of angiogenic factors in malignant melanoma patients correlates with tumor progression and survival. J Clin Oncol 2001;19:577–83.

Vighi E, Rentsch A, Henning P, Comitato A, Hoffmann D, Bertinetti D, et al. New cGMP analogues restrain proliferation and migration of melanoma cells. Oncotarget 2018;9:5301–20.

Vighi E, Trifunović D, Veiga-Crespo P, Rentsch A, Hoffmann D, Sahaboglu A, et al. Combination of cGMP analogue and drug delivery system provides functional protection in hereditary retinal degeneration. Proc Natl Acad Sci USA 2018;115:E2997–3006.

Wang Y, Chen Y, Wu M, Lan T, Wu Y, Li Y, et al. Type II cyclic guanosine monophosphate-dependent protein kinase inhibits Rac1 activation in gastric cancer cells. Oncol Lett 2015;10:502–8.

Windham PF, Tinsley HN. cGMP signaling as a target for the prevention and treatment of breast cancer. Semin Cancer Biol 2015;31:106–10.

Wu M, Wu Y, Qian H, Tao Y, Pang J, Wang Y, et al. Type II cGMP-dependent protein kinase inhibits the migration, invasion and proliferation of several types of human cancer cells. Mol Med Rep 2017;16:5729–37.

Wu Y, Cai Q, Li W, Cai Z, Liu Y, Li H, et al. Active PKG II inhibited the growth and migration of ovarian cancer cells through blocking Raf/MEK and PI3K/Akt signaling pathways. Biosci Rep 2019;39. BSR20190405. d.

Wu Y, Yuan M, Su W, Zhu M, Yao X, et al. The constitutively active PKG II mutant effectively inhibits gastric cancer development via blockade of EGF/EGFR-associated signaling cascades. Ther Adv Med Oncol 2018;10. 1758834017751635.

Yanagi T, Nagai K, Shimizu H, Matsuzawa SI. Melanoma antigen A12 regulates cell cycle via tumor suppressor p21 expression. Oncotarget 2017;8:68448–59.